Adsorption Measurements of Methane on Activated Carbon in the Temperature Range (281 to 343) K and Pressures to 1.2 MPa

Xiaolin Wang,[†] James French,[†] Srinivasan Kandadai,[‡] and Hui Tong Chua*,[†]

School of Mechanical Engineering M050, The University of Western Australia, and Western Australian Geothermal Centre of Excellence, 35 Stirling Highway, Crawley WA 6009, Australia, and Department of Mechanical Engineering, University of Melbourne, VIC 3010, Australia

The adsorption characteristics of methane on a Maxsorb II specimen of activated carbon were measured over the temperature range of (281 to 343) K and at pressures up to 1.2 MPa using a new volumetric measurement system. The adsorbent was characterized through properties such as the skeletal density, Brunauer−Emmett−Teller (BET) surface area, and pore-size distribution. The adsorption data were fitted to two isotherm models proposed by Tóth and Dubinin−Astakhov with a predictive accuracy of better than 3 %. The present data were compared with those of various researchers with comparable specimens and found to be consistent with those in the open literature. The present data could complement efforts in designing adsorbed natural gas storage systems.

Introduction

The present concern on the high rate of greenhouse gas emissions mainly propelled by fossil fuels, such as coal used for power generation and oil used for transportation, requires redressing. Renewable energies, though promising, need to be developed a lot before they can be used in the power and transport sectors at the current level of need. With the discovery of abundant natural gas reserves in several parts of the world, in the coming decades it could be a dominant source of energy for both sectors.[1] However, because a large fraction of it is methane, it suffers from lower volumetric energy density compared with conventional fuels. Hence, its compression and storage are of great interest to industrial and scientific communities. The current methods are storage either in the compressed form (CNG) at pressures of the order of 20 MPa or in the liquefied state (LNG) at temperatures down to 120 K. The latter form is mainly used for intercontinental transportation. There are three alternative technologies for the necessary development of lighter on-board gas storage: (i) the use of suitable solvents, which is disadvantaged by the low solubility of methane implying the need for very high pressure,[2] (ii) the formation of clathrates,[3] which is bogged down by low storage capacity, and (iii) adsorbed natural gas (ANG) storage on a suitable microporous material such as activated carbons.[4]

ANG technology can provide adequate energy density at a moderate pressure of the order of 3.5 MPa (much lower than in CNG) and at room temperature (much higher than LNG), albeit with a corresponding sacrifice in storage capacity. The disadvantage is a poor specific mass (ratio of useful gas stored to total parasitic mass of activated carbon and the container). Yet, it can be construed as an alternative for the transport sector and remote area gas storage provided that higher than 160 (v/v) in volumetric storage capacity can be realized.[5] To overcome the specific mass lacuna, a number of researchers have focused on methane adsorption on microporous activated carbons as adsorbents, such as those from the Maxsorb family and AX21 which are endowed with large specific surface areas.[5–12] Considerable effort was also put into achieving high packing densities.[13,14] Among the methods used for measurements, the volumetric method seems to be the most cost-effective and reliable one because of small error bands associated with it.[15–17]

This paper is complementary to the above efforts to generate data using a constant-volume-variable-pressure (CVVP) apparatus to measure methane adsorption characteristics on solid adsorbents. The main source of uncertainty in the volumetric method is due to the calculation of the amount of adsorbate trapped in the dead volume. The present apparatus estimates this precisely using the helium method which has virtually no adsorption on activated carbon in the temperature and pressure range studied. The isotherms were modeled with the Tóth and Dubinin−Astakhov equations. Isosteric heats of adsorption were derived.

Experimental Section

Characterization of the Adsorbent. The Maxsorb II specimen studied here is the same as that by Akkimaradi et al.,[18] which was manufactured by the Kansai Coke Company. Its surface morphologies were examined by a scanning electron microscope (VPSEM ZEISS 1555). The SEM pictures are shown in Figure 1. The true density of the specimen was measured using a helium pycnometer (Micromeritics AccuPyc 1330) after degassing at 413 K for 8 h. The helium gas used was 99.995 % pure, and the sample was tested for 20 runs yielding an average density of 2.48 $g \cdot cm^{-3}$ with a standard deviation of 0.017 $g \cdot cm^{-3}$. The bulk density could then be easily determined by the weight of the dried Maxsorb sample and its geometrical volume. Nitrogen isotherms were determined at 77 K by using a Micromeritics Gemini 2375 analyzer. The experimental data were analyzed with commercial software (DataMaster) in which the density functional theory (DFT) analytical method was used to determine the pore size distribution and the BET equation was used

* Author to whom correspondence should be addressed. E-mail: htchua@mech.uwa.edu.au.
[†] School of Mechanical Engineering M050, The University of Western Australia, and Western Australian Geothermal Centre of Excellence.
[‡] University of Melbourne.

10.1021/je900959w
Published on Web 03/10/2010

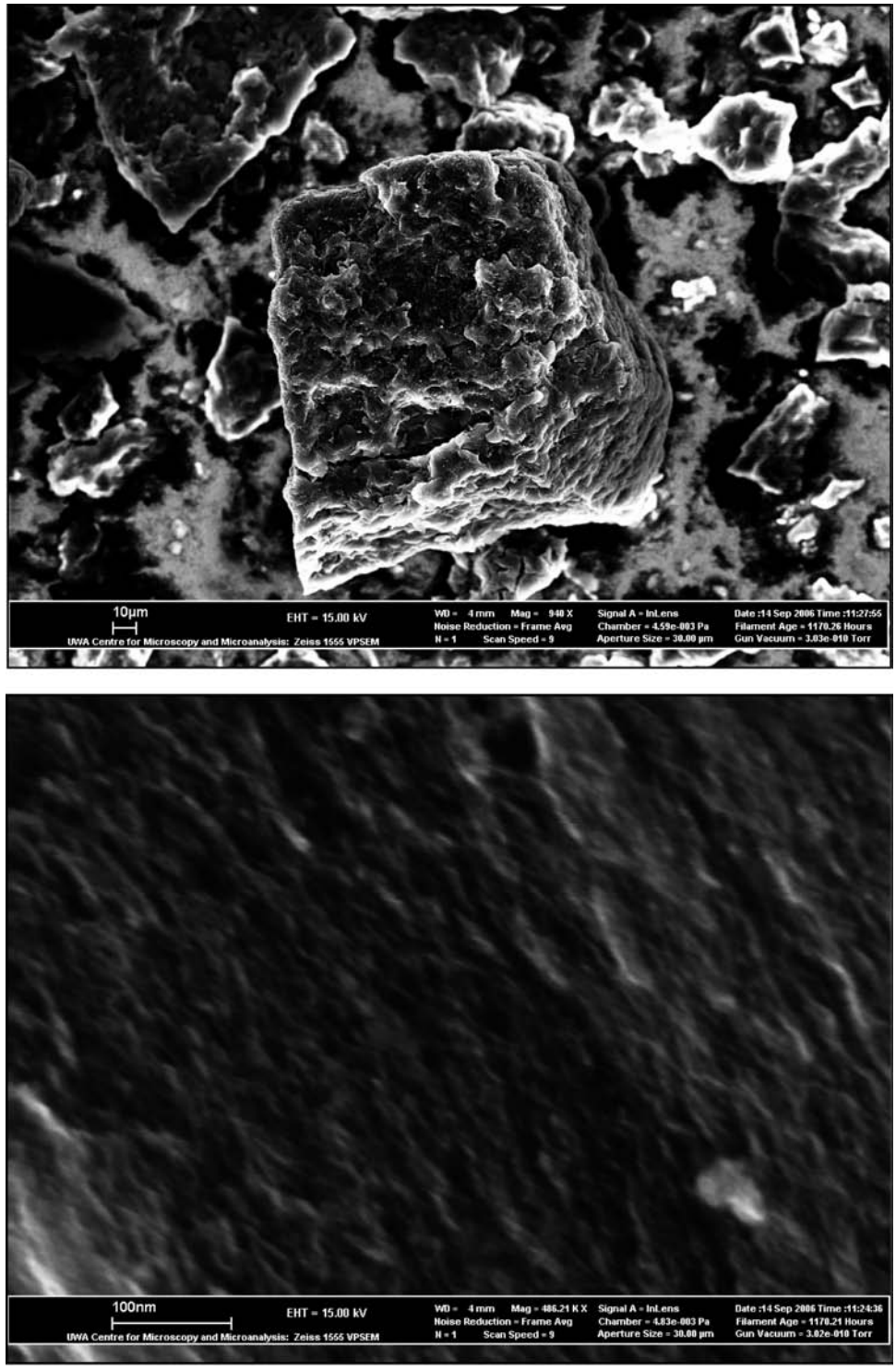

Figure 1. SEM images of Maxsorb II specimen of activated carbon powder (10 μm and 100 nm scale).

to calculate the surface area. A significant volume of pores was in the micropore range (< 2 nm) with the majority being at the lower end of the mesopore range [(2 to 5) nm]. The pore size distribution is shown in Figure 2, which is comparable to reported values in the literature.[8,12,19] The pore volume is 1.38 $cm^3 \cdot g^{-1}$, and Brunauer−Emmett−Teller (BET) surface area of 2768 $m^2 \cdot g^{-1}$ is comparable to the surface areas of a few other Maxsorb species (e.g., 3250 $m^2 \cdot g^{-1}$ for Maxsorb III,[8] 3106 $m^2 \cdot g^{-1}$ for AX21,[10] and 3000 $m^2 \cdot g^{-1}$ for PX21[19]).

Experimental Apparatus. A purpose-built CVVP apparatus as shown in Figure 3 is similar to the one used for the silica gel + water system operating under subatmospheric pressures.[20–22] The modified design of the present apparatus makes it adaptable to high pressures up to 5 MPa. The present CVVP setup consists of a dosing vessel with a volume of (147.4 ± 1.8) cm^3 and a adsorption vessel with a volume of (52.6 ± 0.9) cm^3. Both vessels are constructed from SS316, and their volumes are inclusive of related piping and valves. The volumes of both vessels had been calibrated by charging helium with a purity of 99.995 % from a calibrated standard volume of 493.6 cm^3. This standard volume was calibrated by a liquid filling method from a buret using distilled water. The pressures in the two vessels were monitored by two calibrated digiquartz pressure transducers supplied by Paroscientific [31 K, (0 to 7) MPa span,

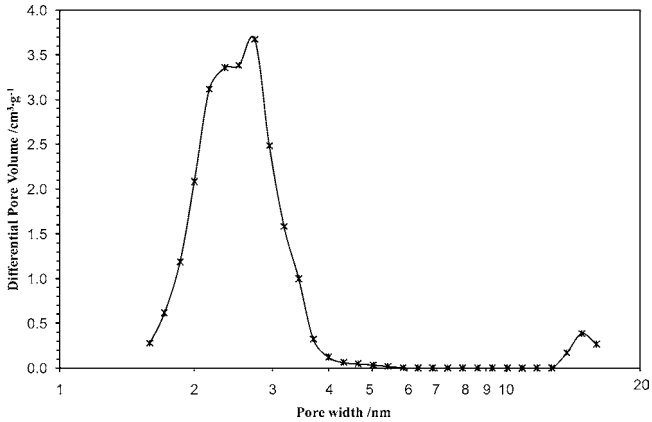

Figure 2. Pore size distribution of Maxsorb II specimen of activated carbon powder.

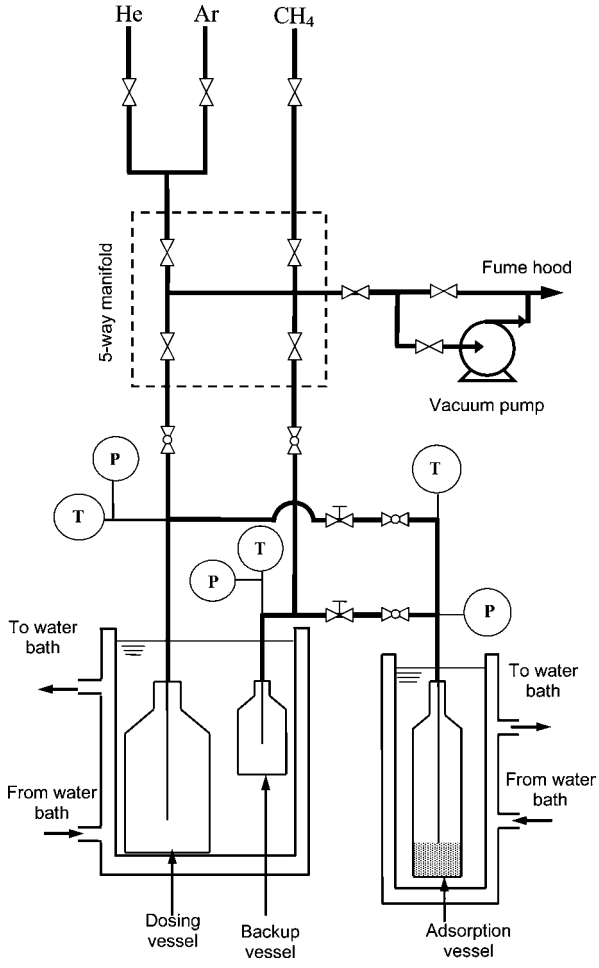

Figure 3. Schematic of the experimental setup.

0.01 % of full scale accuracy, 0.0001 % resolution]. The temperatures were measured with two PT100 class A resistance temperature devices (RTDs). The RTD for the adsorption vessel was designed to be in direct contact with the sample so that the correct representative adsorbent temperature can be measured. All of the pressure and temperature readings were continuously monitored by a calibrated 18-bit ADDA data logger (Fluka Netdaq 2640A). The calibration of pressure transducers, temperature sensors, and the data logger were traceable to relevant international standards. All of the interconnecting piping, valves, and fittings used in the system were standard Swagelok fittings compatible with high pressures.

To maintain the vessels at isothermal conditions and accurately control the temperatures in the vessels, the two vessels were immersed in two individually jacketed housings so that their temperatures could be controlled by the circulation of distilled water from a pair of Thermo Scientific Haake water baths of cooling/heating power capacity of 2 kW. Both units were controlled with a DC50 proportional-integral-derivative (PID) controller with a measurement uncertainty of ± 0.01 K. The operational temperature ranges from (0 to 100) °C. A HTM Reetz tube furnace was used for regeneration. During regeneration, this furnace replaced the adsorption side circulation bath. The furnace is rated up to 500 °C and is PID-controlled to the nearest degree. The sample temperature was monitored by the RTD inserted into the adsorption vessel.

The CVVP setup was evacuated with a two-stage rotary vane vacuum pump (Edwards bubbler pump) with a water vapor pumping rate of $315 \cdot 10^{-6}$ $m^3 \cdot s^{-1}$. To prevent back migration of oil mist, an alumina-packed foreline trap is installed immediately upstream of the vacuum pump. Argon with a purity of 99.995 % was sent through an inline purifier before being used to purge the system.

The dry mass of the Maxsorb II samples was determined with a calibrated moisture analyzer (Satorious MA45, uncertainty 0.05 %, traceable to a DKV standard) at 453 K. The sample mass was continuously monitored and only recorded when no change in mass was detected.

Experimental Procedures

Regeneration. After the Maxsorb II sample was loaded into the adsorption vessel, the test system (dosing and adsorption vessels plus all related piping systems) were first purged by pure and dry argon, evacuated, and subsequently isolated. Thereafter, the Maxsorb II sample was regenerated in situ at 483 K for 8 h, and then the test system was evacuated. The system was again purged with pure dry helium to 100 Pa. On the basis of measurements involving only helium and Maxsorb II samples, it was concluded that there was no measurable interaction between the inert gas and the adsorbent. The effect of the partial pressure of helium in the vessels was found to be very small.[23]

Helium Calibration. Helium was used to calibrate the free space (dead volume or empty volume after the sample was loaded) in the adsorption vessel after the sample had been appropriately regenerated. Helium calibration determines the relationship between the moles of gas in the free space versus the pressure in the adsorption vessel. As helium is not adsorbed at pressures below 10 MPa,[23] this relation is an important measure to determine the moles of methane occupying the free space when measuring adsorption isotherms. Prior to helium charging, the temperature of the dosing vessel was maintained at room temperature (~ 298 K), while the temperature of the adsorption vessel was adjusted to the desired isotherm temperature. Helium (purity 99.995 %) was charged into the dosing vessel from an external supply cylinder via a VICI helium purifier (up to 99.9995 %) along the gas line. Once the dosing vessel reached thermodynamic equilibrium, the temperature and pressure in the vessel were recorded for calculating the amount of helium present, and the globe valve interconnecting the dosing vessel and adsorption vessel was then opened. The helium gas was then charged into the adsorption vessel via a needle valve so that the amount of gas transfer could be controlled. After the two vessels returned to thermal equilibrium, the conditions at both sites were recorded for calculating the amount of helium gas in the adsorption vessel at the relative pressure. By repeating

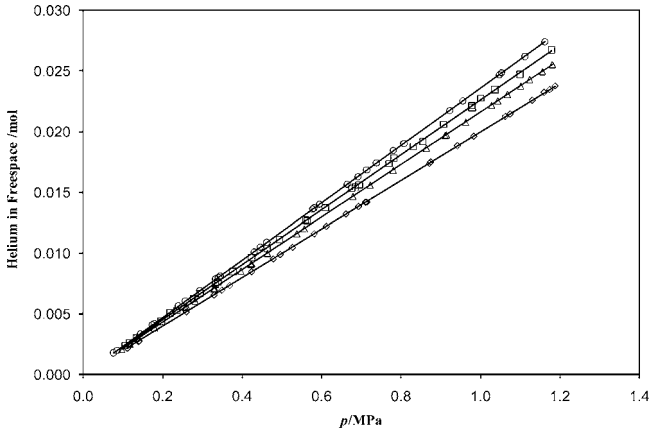

Figure 4. Helium calibration curves at different temperatures. ○, 281 K; □, 298 K; △, 313 K; ◇, 343 K.

this charging process, the amount of helium gas in the adsorption vessel could be worked out at different pressures so that a helium isotherm could be measured. By repeating the whole process (evacuation, regeneration, charging), the helium isotherm at different temperatures was then measured. For each helium isotherm, the test was repeated at least three times to minimize systematic errors.

Methane Isotherm Measurements. The system was evacuated after helium calibration, and the sample was regenerated at 483 K for 8 h to ensure that no residual gases were present in the sample. Prior to charging, the temperature in the dosing vessel was maintained at ~ 298 K while the temperature in the adsorption vessel was maintained at the desired isotherm temperature. The methane (ultra high purity, 99.997 %) was first purified by a VICI methane purifier (up to 99.9995 %) along the gas line and then charged into the dosing vessel. The methane isotherm measurement is similar to that of the helium isotherm measurement with the exception of the adsorption vessel needing a longer duration to achieve thermal equilibrium mainly due to the process of adsorption and heat generated during the process.

Data Reduction. The fluid properties were calculated using equations of state as implemented in REFPROP 7.[24] The uncertainties for gas density at the experimental conditions were 0.1 % for helium and 0.03 % for methane.[25,26] Prior to the calculation of methane adsorbed by the Maxsorb II sample, the amount of methane in the free space must be determined. This was calculated from the helium calibration at the desired adsorption temperature. When the helium was dosed from the dosing vessel into the adsorption vessel loaded with sample, the amount (moles) of helium gas transferred was given by

$$n_{\text{void-He}}(p_a, T_{ad}) = \sum_{i=1}^{N} [\rho_{1-\text{He}}(p_1, T_d) - \rho_{2-\text{He}}(p_2, T_d)]V_d \quad (1)$$

where p_a is the pressure in the adsorption vessel and p_1 and p_2 are the thermal equilibrium pressures in the dosing vessel before and after dosing. T_d and T_{ad} are the set temperature in the dosing vessel and desired adsorption temperature, respectively, ρ_1 and ρ_2 are the densities in the dosing vessel before and after each dose, and V_d is the calibrated volume of the dosing vessel. The summation is over N number of doses before the desired pressure in the adsorption vessel is achieved. The amount of helium transferred is the same as the amount of helium in the free space. By repeating the helium dosing process, the moles of helium in the free space at different pressures could be obtained.

The helium-based dead volume gas moles were scaled to derive corresponding values for methane prediction via a correction factor k, defined as

Table 1. Experimental Isotherms of Methane Adsorption on the Maxsorb II Specimen

p	T	C	p	T	C
MPa	K	g·g^{-1}	MPa	K	g·g^{-1}
0.098	281.37	0.021	0.145	298.23	0.021
0.204	281.41	0.039	0.232	298.20	0.032
0.297	281.44	0.053	0.347	298.19	0.044
0.388	281.44	0.064	0.441	298.18	0.053
0.495	281.44	0.076	0.569	298.15	0.064
0.656	281.46	0.092	0.695	298.14	0.074
0.798	281.45	0.104	0.813	298.12	0.082
0.876	281.42	0.110	0.919	298.09	0.089
0.969	281.40	0.117	1.202	298.06	0.105
1.052	281.39	0.123	1.202	298.23	0.105
1.191	281.38	0.131	0.101	298.20	0.015
0.106	281.37	0.022	0.175	298.19	0.025
0.211	281.37	0.040	0.234	298.18	0.032
0.302	281.57	0.053	0.292	298.15	0.039
0.395	281.48	0.065	0.343	298.14	0.045
0.490	281.43	0.076	0.397	298.12	0.050
0.608	281.48	0.087	0.453	298.09	0.055
0.717	281.41	0.097	0.492	298.06	0.059
0.797	281.42	0.104	0.525	297.66	0.062
0.850	281.38	0.109	0.644	297.75	0.072
0.941	281.36	0.116	0.719	297.81	0.078
0.991	281.36	0.119	0.778	297.82	0.083
1.113	281.73	0.127	0.078	297.83	0.012
1.189	281.66	0.131	0.157	297.83	0.023
0.360	281.63	0.061	0.254	297.86	0.035
0.489	281.59	0.076	0.368	297.86	0.048
0.582	281.53	0.086	0.460	297.88	0.056
0.685	281.52	0.096	0.559	297.84	0.065
0.740	281.49	0.101	0.687	297.86	0.076
0.808	281.49	0.104	0.876	297.86	0.089
0.926	281.42	0.114	0.979	298.06	0.096
1.027	281.40	0.122	1.077	298.00	0.102
1.096	281.41	0.128	1.145	297.98	0.107
0.073	281.35	0.016	1.254	297.97	0.113
			0.084	297.97	0.013
			0.225	297.96	0.032
0.104	313.02	0.012	0.194	343.09	0.013
0.196	313.17	0.022	0.438	343.09	0.028
0.293	313.28	0.031	0.595	342.99	0.036
0.398	313.31	0.040	0.814	342.82	0.047
0.496	313.31	0.048	0.981	342.92	0.055
0.587	313.27	0.052	1.157	342.97	0.063
0.767	313.16	0.064	0.112	343.40	0.008
0.887	313.12	0.072	0.241	343.40	0.017
1.025	313.09	0.081	0.344	343.29	0.024
1.128	313.10	0.086	0.513	342.87	0.034
0.155	313.21	0.017	0.626	342.65	0.041
0.303	313.21	0.032	0.060	343.10	0.004
0.375	313.20	0.038	0.140	343.05	0.010
0.462	313.19	0.045	0.276	343.02	0.019
0.559	313.17	0.052	0.362	342.91	0.024
0.699	313.16	0.062	0.433	342.84	0.028
0.894	313.12	0.074	0.523	342.66	0.033
1.029	313.12	0.082	0.523	342.65	0.034
1.115	313.10	0.087	0.758	342.52	0.045
1.187	313.09	0.091	1.229	342.69	0.066
0.106	313.12	0.012	0.759	342.67	0.043
0.229	313.12	0.025	0.941	342.81	0.052
0.304	313.15	0.032	1.063	342.93	0.057
0.417	313.15	0.042	1.219	343.00	0.064
0.533	313.14	0.050			
0.671	313.12	0.060			
0.816	313.05	0.070			
1.027	313.04	0.082			
1.171	313.05	0.090			
0.753	313.24	0.063			
0.910	313.16	0.072			
1.054	313.16	0.080			
1.232	313.17	0.089			

$$k = \frac{n_{CH_4}}{n_{He}} = \frac{\rho_{CH_4}}{\rho_{He}} \quad (2)$$

k can be calculated and applied at each storage point by evaluating the densities of methane and helium at every observed temperature and pressure.

Figure 4 shows the moles of helium in the system under different measurement temperatures. Since helium is essentially not being adsorbed, a linear relation is evident. Therefore, the methane in the free space at a different pressure could be obtained through these helium curves after correction with the k factor.

The amount of methane leaving the dosing vessel could be calculated from the difference in the densities of the methane in the dosing vessel at two successive pressure and temperature readings (initial, i, and final, f) under thermal equilibrium conditions. The total amount of methane transferred at the desired adsorption pressure, p_a, is given by

$$n_v = \sum_{i=1}^{N} [\rho_i(p_i, T_d) - \rho_f(p_f, T_d)]V_d \quad (3)$$

The amount of methane adsorbed can then be calculated from

$$n_{ad}(p_a) = n_v(p_a, T_{ad}) - k(p_a, T_{ad}) \cdot n_{void-He}(p_a, T_{ad}) \quad (4)$$

The specific adsorbance, C, was given by

$$C = \frac{n_{ad}}{m_{ms}} \quad (5)$$

where m_{ms} is the mass of the adsorbent in the adsorption vessel. Table 1 lists the primary data. The overall uncertainty in C was estimated to be no more than 3 % which was due to the uncertainties in the calibrated volume, the mass of adsorbent, pressure and temperature measurements, and the equation of state.

Isotherm Correlations

The experimental isotherms were correlated with two models, namely, the Tóth and the Dubinin−Astakhov (D−A) equations. Both of them have been widely used for IUPAC Type 1 isotherms which are typical of physisorption of several gases on activated carbons.[12,27] The form of the Tóth equation used herein is given below:

$$C = \frac{C_m k_o \exp\left(\frac{\Delta h_{st}}{RT}\right)p}{\{1 + [k_o \exp\left(\frac{\Delta h_{st}}{RT}\right)p]^t\}^{1/t}} \quad (6)$$

where k_o is the pre-exponential constant, Δh_{st} the isosteric heat of adsorption, R the universal gas constant, p and T the equilibrium pressure and temperature of the adsorbate in the gas phase, C_m denotes the monolayer adsorption capacity, and t is the dimensionless Tóth constant, which is a measure of structural heterogeneity of adsorbent micropores. k_o, C_m, and Δh_{st} are the adsorption parameters that are optimized from the least-squares criteria using the experimental data in Table 1.

The D−A equation has the following form

$$W = W_0 \exp\left[-\left[\frac{RT}{E}\ln\left(\frac{p_s}{p}\right)\right]^n\right] \quad (7)$$

where

Table 2. Adsorption Isotherm Parameters for Tóth and D−A Equations

	Tóth	D−A
C_0/g·g^{-1}	0.400	
$(\Delta h_{st}/R)$/K	1844	
k_o/MPa^{-1}	$9.4 \cdot 10^{-4}$	
n or t	0.707	1.2
W_0/cm^3·g^{-1}		1.409
E/J·mol^{-1}		4548
α/K^{-1}		1/446
average error deviation/g·g^{-1}	$1.0 \cdot 10^{-3}$	$1.6 \cdot 10^{-3}$

$$W = C\nu_a \quad (8)$$

In the above equations, ν_a is the adsorbed phase specific volume which is calculated as follows:[12]

$$\nu_a = \nu_b \exp[\alpha(T - T_b)] \quad (9)$$

where the subscript b refers to the normal boiling point in the liquid state. The index n denotes the structural heterogeneity factor (similar to t in the Tóth equation). Since all of the measurements here are above the critical point of methane, the pseudosaturation pressure (p_s) is calculated as follows:

$$p_s = (T/T_c)^2 p_c \quad (10)$$

where the subscript c refers to the critical point. In this case W_0, E, and n are the adsorption parameters which are optimized from the least-squares criteria. The methodology used in applying the least-squares criteria is the same as that described in ref 27.

Results and Discussion

The fitting parameters of the isotherms and relative average deviations are shown in Table 2. The experimental data and the fits with the two isotherms are shown in Figure 5. The deviation plots for the two isotherms are given in Figure 6. In the D−A isotherm the parameter designating the thermal expansion of the adsorbed phase specific volume (α in eq 9) is found to be 1/446 K^{-1} as against 1/400 K^{-1} used by Himeno et al.[8] and $1/T$ used by Saha et al.[12] It is seen that the D−A equation is associated with larger positive deviations than the Tóth equation in the 0.04 g·g^{-1} and negative deviations in the 0.10 g·g^{-1} uptake region indicating that the curvature of the isotherm in the lower temperatures is not exactly reproduced. Yet, both of the isotherms reproduce the experimental data within the estimated uncertainty of 3 %. Figure 7 compares the

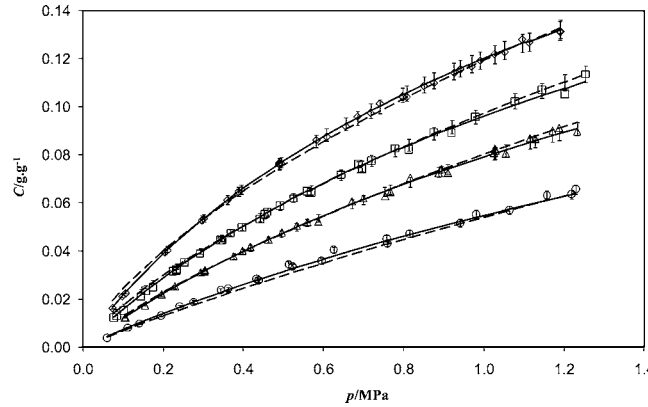

Figure 5. Isotherms of methane adsorption on Maxsorb II. ◇, 281 K; □, 298 K; △, 313 K; ○, 343 K; full line, Tóth isotherm; broken line, D−A isotherm.

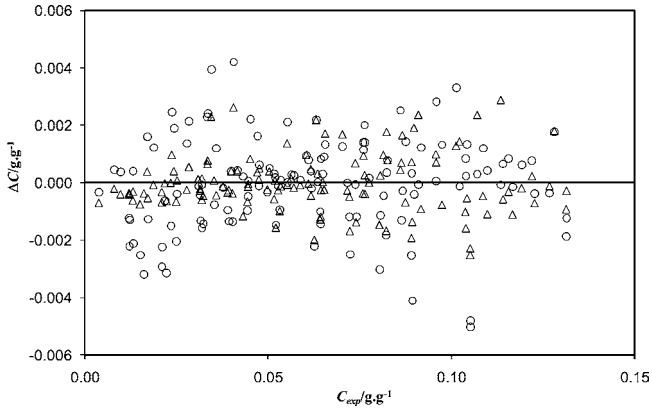

Figure 6. Deviation plots for Tóth and D−A isotherms. △, Tóth; ○, D−A.

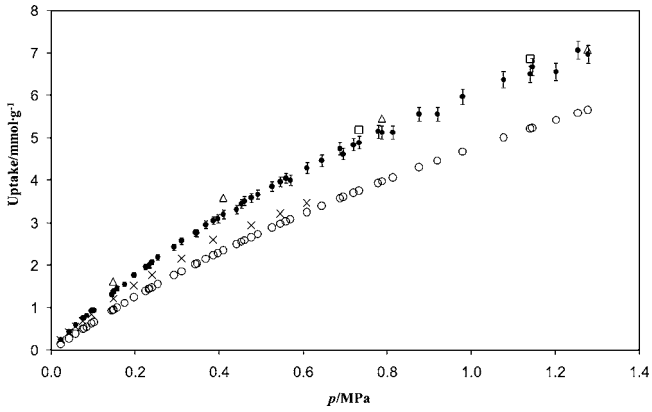

Figure 7. Comparison of methane uptake data with other specimens of activated carbon of comparable surface area. ●, present data at 298 K; ○, Saha et al.[12] at 298 K; ×, Sheikh et al.[6] at 300 K; △, Zhou et al.[9] at 293 K; □, Himeno et al.[7] at 298 K.

uptake by other similar high surface area adsorbents, which calibrates the present apparatus.

The uptake dependence of the isosteric heat of adsorption is calculated using the following equation which can be obtained by applying the Clausius−Clapeyron equation to the D−A isotherm:[27]

$$\Delta h_{st} = 2RT + E\left[\left(\ln\left(\frac{W_0}{Cv_a}\right)\right)^{1/n}\left\{1 + \frac{\alpha T_b/n}{\ln\left(\frac{W_0}{Cv_a}\right)}\right\}\right] \quad (11)$$

Figure 8 shows the relative uptake dependence of this property. This is a useful piece of information since the Tóth isotherm assumes a constant value for it. Although there is only a marginal temperature dependence, following Akkimaradi et al.,[27] the isosteric heat of adsorption has been correlated as given below:

$$\Delta h_{st}/\mathrm{J\cdot mol^{-1}} = \Delta h_{st0} - \beta \ln(C/C_0) \quad (12)$$

with

$$\Delta h_{st0}/\mathrm{J\cdot mol^{-1}} = 506.1 + 22.89(T/\mathrm{K}) \quad (13)$$

$$\beta = 4053 - 2.63(T/\mathrm{K}) \quad (14)$$

In eq 12, since $C_0 = W_0/v_a$, it will be different for each isotherm due to a variation of the adsorbed phase specific volume with temperature. On the other hand, the D−A isotherm does not

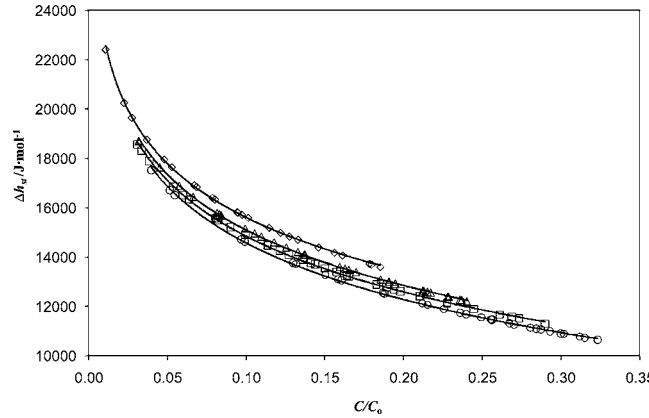

Figure 8. Uptake dependence of isosteric heat of adsorption derived from D−A isotherm. ○, 281 K; □, 298 K; △, 313 K; ◇, 343 K.

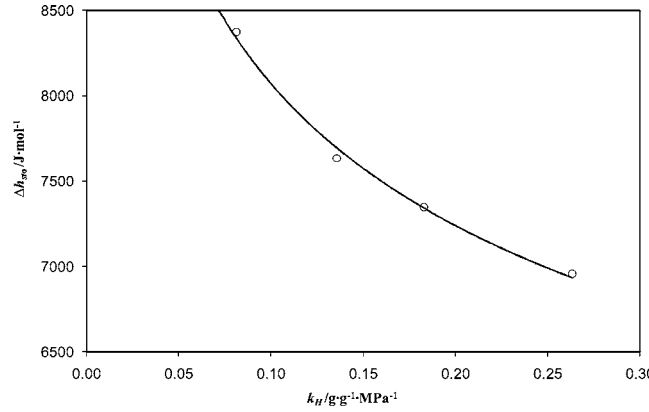

Figure 9. Relation between Henry's law coefficients and the isosteric heat of adsorption at monolayer coverage.

have a Henry's law regime (dC/dp as $p \rightarrow 0$), and Henry's law coefficients can be calculated readily from the Tóth isotherm.

$$k_H = \lim_{p\to 0}\left(\frac{\partial C}{\partial p}\right)_T = C_0 k_0 \exp\left(\frac{\Delta h_{st}}{RT}\right) \quad (15)$$

Along an isotherm, the Henry's law coefficients (k_H) at the lower end of the uptake derived from the Tóth isotherm and the limiting isosteric heat of adsorption at the maximum monolayer coverage (Δh_{st0}) derived from the D−A equation were linked by Akkimaradi et al.[27] for nitrogen. Figure 9 shows that a similar analogy holds for methane too, with the following empirical correlation:

$$\Delta h_{st0}/\mathrm{J\cdot mol^{-1}} = 5626(k_H/\mathrm{g\cdot g^{-1}\cdot MPa^{-1}})^{-0.157} \quad (16)$$

Conclusion

A purpose-built high-pressure compatible CVVP apparatus was used for the measurement of fairly precise adsorption equilibrium data for methane on a Maxsorb II specimen of activated carbon, over the temperature range (281 to 343) K and pressures up to 1.2 MPa. A good agreement between these data and from the literature on comparable adsorbents was observed which validates the apparatus and the technique. The data were fitted to the Tóth and Dubinin−Astakhov equations applicable for IUPAC Type 1 adsorption. The isosteric heats of adsorption and Henry's law coefficients could be obtained from the present data. A link between them has been established.

Acknowledgment

We gratefully acknowledge the assistance of Ceasar Wood, Andrew Plavina, Benjamin Lee, and the CVVP student team for collecting

a comprehensive set of data. We also acknowledge the facilities and scientific and technical assistance of the Australian Microscopy & Microanalysis Research Facility at the Centre for Microscopy, Characterisation & Analysis, The University of Western Australia, a facility funded by The University, State and Commonwealth Governments.

Literature Cited

(1) Parkyns, N. D.; Quinn, D. F. In *Porosity in Carbons*; Patrick, J. W., Ed.; Edward Arnold: London, 1995; p 291−325; Chapter *11*.

(2) Wang, L.; Gardeler, H.; Gmehling, J. Model and experimental data research of natural gas storage for vehicular usage. *Sep. Purif. Technol.* **1997**, *12*, 35–41.

(3) Yevi, G. Y.; Rogers, R. E. Storage of fuel in hydrates for natural gas vehicles (NGVs). *J. Energy Resour. Technol.* **1996**, *118*, 209–213.

(4) Wegrzyn, J.; Gurevich, M. Adsorbent storage of natural gas. *Appl. Energy* **1996**, *55*, 71–83.

(5) Lozano-Castelló, D.; Cazorla-Amorós, D.; Linares-Solano, A. Powdered activated carbons and activated carbon fibers for methane storage: A comparative study. *Energy Fuels* **2002**, *16*, 1321–1328.

(6) Sheikh, M. A.; Hassan, M. M. I.; Laughlin, K. F. Adsorption equilibria and rate parameters for nitrogen and methane on Maxsorb activated carbon. *Gas Sep. Purif.* **1996**, *10*, 161–168.

(7) Himeno, S.; Komatsu, T.; Fujita, S. Development of a new effective biogas adsorption storage technology. *Adsorption* **2005**, *11*, 899–904.

(8) Himeno, S.; Komatsu, T.; Fujita, S. High pressure adsorption equilibria of methane and carbon dioxide on several activated carbons. *J. Chem. Eng. Data* **2005**, *50*, 369–376.

(9) Zhou, L.; Zhou, Y.; Li, M.; Chen, P.; Wang, Y. Experimental and modeling study of the adsorption of supercritical methane on a high surface activated carbon. *Langmuir* **2000**, *16*, 5955–5659.

(10) Zhou, L.; Ming, L.; Zhou, Y. Measurement and theoretical analysis of the adsorption of supercritical methane on super activated carbon. *Sci. China, Ser. A* **2000**, *43*, 143–153.

(11) Wu, J.; Zhou, L.; Sun, Y.; Su, W. Measurement and prediction of adsorption equilibrium for a $H_2/N_2/CH_4/CO_2$ Mixture. *AIChE J.* **2007**, *53*, 1178–1191.

(12) Saha, B. B.; Koyama, S.; El-Sharkawy, I. I.; Habib, K.; Srinivasan, K.; Dutta, P. Evaluation of adsorption parameters and Heats of adsorption through desorption measurements. *J. Chem. Eng. Data* **2007**, *52*, 2419–2424.

(13) MacDonald, J. A. F.; Quinn, D. F. Carbon adsorbents for natural gas storage. *Fuel* **1998**, *77*, 61–64.

(14) Biloe, S.; Goetz, V.; Mauran, S. Characterization of adsorbent composite blocks for methane. *Carbon* **2001**, *39*, 1653–1662.

(15) Malbrunot, P.; Vidal, D.; Vermesse, J.; Chahine, R.; Bose, T. K. Adsorption measurements of argon, neon, krypton, nitrogen, and methane on activated carbon up to 650 MPa. *Langmuir* **1992**, *8*, 577–580.

(16) Choi, B. K.; Choi, D. K.; Lee, Y. W.; Lee, B. K.; Kim, S. H. Adsorption equilibria of methane, ethane, ethylene, nitrogen and hydrogen onto activated carbon. *J. Chem. Eng. Data* **2003**, *48*, 603–607.

(17) Belmabkhout, Y.; De Weireld, G.; Frère, M. High-pressure adsorption isotherms of N_2, CH_4, O_2, and Ar on different carbonaceous adsorbents. *J. Chem. Eng. Data* **2004**, *49*, 1379–1391.

(18) Akkimaradi, B. S.; Prasad, M.; Dutta, P.; Srinivasan, K. Adsorption of 1,1,1,2-tetrafluoroethane on actovated charcoal. *J. Chem. Eng. Data* **2001**, *46*, 417–422.

(19) Sosin, K. A.; Quinn, D. F. Using the high pressure methane isotherm for determination of pore size distribution of carbon adsorbents. *J. Porous Mater.* **1995**, *1*, 111–119.

(20) Chua, H. T.; Ng, K. C.; Chakraborty, A.; Oo, N. M.; Othman, M. A. Adsorption characteristics of silica gel + water systems. *J. Chem. Eng. Data* **2002**, *47*, 1177–1181.

(21) Wang, X.; Zimmermann, W.; Ng, K. C.; Chakraborty, A. Investigation on the isotherm of silica gel + water systems by using TG and volumetric methods. *J. Therm. Anal. Calorim.* **2004**, *76*, 659–669.

(22) Ng, K. C.; Chua, H. T.; Chung, C. Y.; Loke, C. H.; Kashiwagi, T.; Akisawa, A.; Saha, B. B. Experimental investigation of the silica gel-water adsorption isotherm characteristics. *Appl. Therm. Eng.* **2001**, *21*, 1631–1642.

(23) Malbrunot, P.; Vidal, D.; Vermesse, J. Adsorbent helium density measurement and its effect on adsorption isotherms at high pressure. *Langmuir* **1997**, *13*, 539–544.

(24) Lemmon, E. W.; McLinden, M. O.; Huber, M. L. *REFPROP 7. Reference Fluid Thermodynamic and Transport Properties*; National Institute of Science and Technology: Gaithersburg, MD, 2002.

(25) McCarty, R.; Arp, V. A new wide range equation of state for helium. *Adv. Cryog. Eng.* **1990**, *35*, 1465–1475.

(26) Setzmann, U.; Wagner, W. A new equation of state and tables of thermodynamic properties for methane covering the range from the melting line to 625 K at pressures up to 1000 MPa. *J. Phys. Chem. Ref. Data* **1991**, *20*, 1061–1155.

(27) Akkimaradi, B. S.; Prasad, M.; Dutta, P.; Saha, B. B.; Srinivasan, K. Adsorption of nitrogen on activated carbon-refit of experimental data and derivation of properties required for design of equipment. *J. Chem. Eng. Data* **2009**, *46*, 2291–2295.

Received for review November 9, 2009. Accepted February 5, 2010. We gratefully acknowledge the financial support from the Western Australian Geothermal Centre of Excellence.

JE900959W